Journal of NAMP 71, (2025) 159-172

The Nigerian Association of Mathematical Physics

Journal homepage: https://nampjournals.org.ng

SIMULATION AND ASSESSMENT OF THE EXPERIMENTAL PARAMETERS OF FRACTIONAL-ORDER FOR THIN PLATE VIBRATION DYNAMICS EQUATION

FALADE KAZEEM IYANDA[1*], KOLAWOLE ADEFEMI ADEYEMO[2], SANI NASIRU[3]

[1]*Department of Mathematics, Aliko Dangote University of Science and Technology, Wudil Kano State Nigeria.*
[2]*Department of Computer and Mathematics, Nigeria Police Academy, Wudil Kano State Nigeria*
[3]*Department of Mathematics and Statistics, Kaduna Polytechnics, Kaduna State Nigeria...*

ARTICLE INFO

Article history:
Received xxxxx
Revised xxxxx
Accepted xxxxx
Available online xxxxx

Keywords:
Fractional time-vibration dynamics,
thin plates,
three-dimensional coordinates,
Young's modulus.

ABSTRACT

Fractional vibration dynamics in rectangular thin plates use fractional derivatives to represent material memory and hereditary effects, introducing notable mathematical complexity. This study assesses the experimental parameters and the variation of time-fractional orders to simulate vibration behavior over time. A computational framework developed in Maple is applied to analyze how changes in the fractional order affect vibration frequencies, alongside variations in Young's modulus—a key indicator of material stiffness governing stress–strain relationships. The simulations show that both parameters strongly influence the plate's dynamic response. Increasing the fractional order modifies damping and resonance patterns, while higher values of Young's modulus raise natural frequencies and alter vibrational modes. The results provide valuable insight into how fractional dynamics interact with elastic properties, supporting improved analysis and design of advanced materials and structures exposed to vibration. This approach enhances the modeling of vibration-sensitive engineering systems by accurately capturing complex mechanical behavior.

1 INTRODUCTION

A rectangular thin plate is regarded as a fundamental structural component in numerous real-world engineering applications, ranging from mechanical and aeronautical systems to marine, civil, and structural engineering. Owing to their lightweight profile, high strength-to-weight ratio, and versatility in design, thin plates are extensively used in the manufacturing of aircraft wings, building floors, ship hulls, microelectromechanical systems (MEMS), and many precision instruments. To ensure reliable performance and structural integrity, accurate investigation of their dynamic properties-particularly vibration behavior—is essential. Improper prediction or control of plate vibrations can lead to excessive noise, fatigue, resonance-induced failures, and compromised safety or functionality in engineering systems. Traditionally, the vibration dynamics of thin plates have been analyzed using classical integer-order partial differential equations (PDEs), which assume idealized, memoryless material behavior.

[*]Corresponding author: FALADE KAZEEM IYANDA
E-mail address: faladekazeem2016@kustwudil.edu.ng
https://doi.org/10.60787/jnamp.vol71no.608

However, experimental evidence and advances in material science indicate that many plate materials, especially modern composites and metals exposed to complex environments, exhibit nonlocal, history-dependent properties. Classical models often fail to capture the hereditary and damping effects resulting from internal friction, viscoelasticity, or microstructural phenomena. To bridge this gap, time-fractional derivatives have emerged as powerful modeling tools, enabling the formulation of time-fractional vibration dynamics equations. These fractional models incorporate memory effects, providing a more realistic depiction of how past states influence present vibrations and leading to improved predictions of both transient and steady-state responses [1].

In this article, we consider the vibration dynamics in a rectangular thin plate model of the form [2]

$$\frac{\partial^{\alpha}\phi(\mathrm{x,y,t})}{\partial t^{\alpha}} = \frac{R}{\rho\, h}\left(-2\frac{\partial^{4}\phi(\mathrm{x,y,t})}{\partial x^{2}\partial y^{2}} - \frac{\partial^{4}\phi(\mathrm{x,y,t})}{\partial x^{4}} - \frac{\partial^{4}\phi(\mathrm{x,y,t})}{\partial y^{4}}\right), \qquad 0 < \alpha \leq 2 \qquad (1)$$

Where ϕ is the unknown function, $R = \frac{Eh^{3}}{12(1-\mu^{2})}$ is the elasticity modulus, ρ is the mass density of the plate, h is the uniform thickness and μ is the Poisson's ratio. The mathematical complexity of time-fractional PDEs complicates both their analytical and numerical treatment, particularly when the order of the fractional derivative a parameter that dictates the intensity of memory effects varies or must be tailored for specific materials. Furthermore, material parameters such as Young's modulus, which quantifies the elasticity or stiffness of a plate, profoundly affect its vibration characteristics. Accurately simulating how simultaneous changes in fractional derivative order and Young's modulus influence vibration frequencies, damping, and mode shapes is essential for robust, material-sensitive plate design. This paper investigates how variations in the fractional derivative order affect the vibration response of a rectangular thin plate, specifically its natural frequencies and damping characteristics. It also explores the combined effects of fractional derivatives and experimental material parameters (Aluminium, Brass, Epoxy Glass, and Hard Wood), including Young's modulus E, mass density ρ, and Poisson's ratio μ, under uniform thickness. Understanding these interactions is crucial for improving computational modeling and simulation methods, which can drive advances in designing vibration-optimized materials and engineering structures. However, a comprehensive computational study examining the combined effects of varying the fractional order α and Young's modulus E on vibration responses for common engineering materials remains lacking and this paper aim to fill that gap.

In recent years, several authors have proposed suitable analytic–numeric methods. For example, [3] presented an analytical and experimental investigation on the free vibration of a floating composite sandwich plate with viscoelastic layers; [4] provided analytical buckling solutions for rectangular thin plates using the generalized integral transform method; [5] employed a unified formulation for the free vibration of laminated plates through the Jacobi–Ritz method; [6] studied thin plate vibration using the homotopy perturbation algorithm; [7] applied the Adomian decomposition method to the free vibration analysis of thin isotropic rectangular plates submerged in fluid, [8] presented the mathematical modelling and solution of nonlinear vibration problems in laminated plates with CNT-originating layers on a two-parameter elastic foundation; [9] investigated the poroelastic size-dependent dynamics of viscoelastic microbeams connected through a viscoelastic layer; and [10] examined the nonlinear dynamics and forced vibrations of simply supported fractional viscoelastic microbeams using a fractional differential quadrature method. Existing works largely emphasizes analytical and semi-analytical solutions for thin plate vibrations, yet it insufficiently addresses the effects of experimentally varied fractional-order parameters on vibration responses. This study fills that gap by simulating how changes in the fractional derivative order influence the natural frequencies and damping characteristics of rectangular thin plates, considering the experimental properties of Aluminium, Brass, Epoxy Glass, and Hard Wood, each with distinct Young's modulus, density, Poisson's ratio, and uniform thickness.

Fractional Calculus [11]

Definition 1.

Let $\alpha > 0$ we define the Riemann-Liouville fractional integral by

$$ {}_0^R D_t^{-\alpha}\phi(\mathrm{t}) = \frac{1}{\Gamma(\alpha)}\int_0^t (t-\tau)^{\alpha-1}\phi(\tau)\,d\tau, \qquad \alpha > 0 \qquad (2)$$

Suppose $\alpha = 1,$ then equation (2) reduces to the integral of the form

$$ {}_0^R D_t^{-1}\phi(\mathrm{t}) = \int_0^t \phi(\tau)\,d\tau \qquad \alpha = 1 \qquad (3)$$

Description of the computational technique

In this section, we propose and implement a finite difference scheme using a fractional time-stepping algorithm based on the Riemann–Liouville integral. The method begins by dividing the time domain into uniform intervals of size Δt, enabling a time-marching solution approach. This scheme is well-suited for handling fractional derivatives, allowing precise tracking of the plate's dynamic response over time. The algorithm incorporates the influence of the fractional order α on vibration characteristics, including frequency attenuation and damping effects governed by stiffness, which is affected by changes in Young's modulus—a key indicator of material elasticity. As α varies, the non-local memory effects inherent in fractional calculus modify the plate's behaviour. Maple's symbolic computation tools are used to formulate the governing equations with fractional Riemann–Liouville derivatives, while its numerical solvers facilitate the time-progression of the solution.

Description of the finite difference scheme with a fractional time-stepping algorithm based on the Riemann-Liouville integral

Step 1: Initialization: This first stage goes thus:

Identify and initialize all parameters: Elasticity modulus E, plate thickness h, Poisson's ratio μ, density ρ, and flexural rigidity $R = \frac{Eh^3}{12(1-\mu^2)}$. We define the spatial domain (x, y) and time domain t, and initialize the unknow function $\phi(x, y, t)$ with specific conditions and boundary conditions.

Step 2: Decompose the model equation (1) into the Riemann-Liouville fractional integral (2)

We consider the Riemann-Liouville fractional derivative definition for order α. For the Riemann-Liouville fractional derivative of order α, the operator can be represented as a fractional integral and integer derivative composition:

$$\frac{\partial^\alpha \phi}{\partial t^\alpha} = \frac{\mathrm{d}^n}{\mathrm{d}t^n}(I^{n-\alpha} - \phi) \qquad (4)$$

Where I^β is the Riemann-Liouville fractional integral of order β, and $n = \lceil \alpha \rceil$

By rewriting equation (4), which is equivalent to a fractional integral equation using the Riemann-Liouville fractional integral operator:

$$\phi(\mathrm{x,y,t}) = \phi(\mathrm{x,y,0}) + \frac{R}{\rho\, h} {I_t}^\alpha \left(-2\frac{\partial^4\phi}{\partial x^2 \partial y^2} - \frac{\partial^4\phi}{\partial x^4} - \frac{\partial^4\phi}{\partial y^4}\right) \qquad (5)$$

Where the fractional integral ${I_t}^\alpha$ acts on the right-hand side to the spatial derivatives of ϕ.

Step 3: Evaluate the length of the finite computational steps, N Discretize the time domain into N time steps: $t_0 = 0, t_1, \ldots, t_N = T,$ with step size Δt. The numerical approximation for the Riemann-Liouville fractional integral, which allows evaluating fractional integrals/sums at discrete time steps up to length N and obtaining the fourth-order mixed derivatives.

Step 4: Factorize and collect the like terms

For each time step $n = 1, 2, \ldots, N_t$, and compute the fractional time derivative term using past values of ϕ^m for $m < n$. We assemble the spatial discretize of the operator and form the right - hand side using the previous time step solutions and fractional derivatives. Solve the resulting sparse linear system for ϕ^n using Maple linear solvers.

Step 5: Display the output of the simulations in visualized 2D, 3D surfaces, and appendices.
Store ϕ^n solution at each time step for visualization and Maple plots commands to generate 2D/3D surface plots for $\phi(\mathrm{x},\mathrm{y},t_n)$ at the selected times.
Table 1. Presents a summary of the five-step finite difference scheme with a fractional time-stepping algorithm.

Table 1. Maple codes command Implementation

Step	Description	Mathematical Expression
Step 1: Initialization	Initialize all physical parameter: Elasticity modulus E, plate thickness h, Poisson ratio μ, density ρ, flexural rigidity $R=\frac{Eh^3}{12(1-\mu^2)}$. Define spatial domain $(x,y)\in[0,L_x]\times[0,L_y]$, and time domain $t\in[0,T]$. Set initial and boundary conditions for $\phi(\mathrm{x},\mathrm{y},0)$, $\frac{\partial\phi(\mathrm{x},\mathrm{y},0)}{\partial t}$, and the edge values	$\phi(\mathrm{x},\mathrm{y},0)=f_0(x,y)$ $\frac{\partial\phi(\mathrm{x},\mathrm{y},\mathrm{t})}{\partial t}=g_0(x,y)$ $R=\frac{Eh^3}{12(1-\mu^2)}$
Step 2: Reformulation Using Riemann-Liouville fractional integral	Convert the time-fractional PDE into equivalent fractional integral from the Riemann-Liouville definition. Recast the governing PDE: $\phi(\mathrm{x},\mathrm{y},\mathrm{t})=\phi(\mathrm{x},\mathrm{y},0)+I_t^{\alpha}f(\mathrm{t})$ $=\frac{R}{\rho h}I_t^{\alpha}\left[-2\frac{\partial^4\phi(\mathrm{x},\mathrm{y},\mathrm{t})}{\partial x^2\partial y^2}-\frac{\partial^4\phi(\mathrm{x},\mathrm{y},\mathrm{t})}{\partial x^4}-\frac{\partial^4\phi(\mathrm{x},\mathrm{y},\mathrm{t})}{\partial y^4}\right]$	Apply fractional integral $I_t^{\alpha}f(\mathrm{t})=\frac{1}{\Gamma(\alpha)}\int_0^t(t-\tau)^{\alpha-1}$
Step 3: Discretization	Discretize the time domain $t_n=n\Delta t_n, n=0,1,\ldots,N_t$ Where $\Delta t=\frac{T}{N_t}$, Use finite differences for space and a numerical quadrature scheme to approximate the fractional integral over t. Compute mixed and pure fourth-order spatial derivatives using central differences	For each grid point (i,j) ${\phi^n}_{i,j}={\phi^0}_{i,j}+\frac{R}{\rho h}\Delta t^{\alpha}\sum_{k=0}^{n-1}b_k$
Step 4: Assembly and solution	For each time step n Use known ϕ^m for $m<n$ to compute the time fractional history. Discretize the spatial operator $\Delta^4\phi$. Solve the resulting linear algebraic system for ϕ^n using Maple sparse matric solvers.	Solve linear system $A\phi^n=b$ Where A is the sparse matrix and b include contribution from initial and boundary conditions
Step 5: Postprocessing and visualization	Store the numerical solution $\phi^n(x,y)$ at each time step. Use Maple plotting tools (plot3D, surf data etc) to generate 2D contour plots and 3D surface visualizations for $\phi(x,y,t_n)$.	Outputs: Plot2D $(\phi(x),x=0..1)$ Plot3D $\left(\phi(x,y),x=0..\frac{\cdot\pi}{2},y=0..\frac{\cdot\pi}{2}\right)$

4. Error, Stability Analysis, and Convergence

4.1.1 Error analysis

The error analysis in the fractional-order thin plate vibration models emphasizes the combined influences of fractional derivative discretization, spatial approximation, fractional order memory effects, and material stiffness E on the accuracy and reliability of numerical simulations**.**
Suppose $\phi(x,y,t;\alpha,E)$ is the exact solution and $\phi^{(num)}(x,y,t;\alpha,E)$ is the numerical approximation, then the local truncation error (LTE) is

$$\tau(x,y,t) = \frac{\partial^{\alpha}\phi}{\partial t^{\alpha}}_{exact} - \frac{\partial^{\alpha}\phi}{\partial t^{\alpha}}_{numerical} \quad (6)$$

and the global error at time t_n is

$$e(x,y,t_n) = \phi^{(num)}(x,y,t;\ \alpha,E) - \phi(x,y,t;\ \alpha,E) \quad (7)$$

The maximum absolute error is

$$\|e(t_n)\|_{\infty} = \max_{x,y}\left[\phi^{(num)}(x,y,t_n) - \phi(x,y,t_n)\right] \quad (8)$$

And L_2 norm error is

$$\|e(t_n)\|_2 = \left(\sum_{i,j}\left[\phi^{(num)}(x_i,y_j,t_n) - \phi(x_i,y_j,t_n)\right]^2 \Delta x \Delta y\right)^{\frac{1}{2}} \quad (9)$$

Combining all sources of error is

$$\|e(t_n)\| \le C_1\Delta t^{2-\alpha} + C_2\Delta x^2 + C_3\Delta y^3 + C_4\epsilon_E \quad (10)$$

Where $\epsilon_E = \left[E^{(num)} - E^{(exact)}\right]$ and C_1, C_2, C_3, and C_4 depend on the solution's smoothness, modes, and fractional order.

4.2 Stability Analysis

The stability analysis of fractional-order models for thin plate vibration dynamics reveals how fractional-order derivatives intricately influence vibration frequencies, particularly concerning material parameters like Young's modulus E.

$$\Delta t^{\alpha} \le C\left(\frac{\Delta x^4 \Delta y^4}{R}\right)^{\frac{1}{\alpha}} \quad (11)$$

Where C is the constant depending on the initial and boundary conditions and plate geometry.
The stability of the computational algorithm depends strongly on the fractional order α, time step Δt, and the spatial resolution. As α decreases, the smaller time steps are required to maintain stability.

4.3 Convergence

The convergence of the fractional-order thin plate vibration model is essentially to establish that the numerical or analytical method used to solve the governing fractional PDE is accurate and stable as it approaches the true solution when step sizes go to zero particularly under variations in fractional order α and Young's modulus E.
The frequency spectrum $\omega(\alpha, E)$ shifts with α, and the numerical convergence must account for these changes, Young modulus E affects flexural rigidity since $R = \frac{Eh^3}{12(1-\mu^2)}$, increasing E increases R, thereby increasing vibration frequency ω, leading to faster oscillation.
The convergence refers to whether the numerical solution $\phi^{(num)}(x,y,t)$ approaches the exact solution $\phi^{(exact)}(x,y,t)$ as the mesh sizes $\Delta x, \Delta y, \Delta t \to 0$. For the given algorithm, the convergence depends on consistency and stability. The convergence rate of the computational algorithm is measured by the rate:

$$\mathbb{O}(\Delta t^{2-\alpha} + \Delta x^2 + \Delta y^2) \quad (12)$$

As $\Delta t, \Delta x, \Delta y \to 0$, the numerical solution converges to the exact solution, and convergence is lower for small α.

5. Computational Experiments

In this section, we apply the proposed algorithm to simulate numerical solutions for the four different materials (Aluminium, Brass, Epoxy glass, and wood (hard)) with different Young's modulus, ρ, the mass density of the plate, and μ is Poisson's ratio, while the thickness is uniform

Table 2. Suitable values for the engineering materials [12]

Materials	$E(Pa)$	μ	$\rho(kg/m^3)$	Notes
Aluminium	7.0×10^{10}	0.33	2700	Lightweight
Brass	1.1×10^{11}	0.34	8500	Dense, Moderate stiffness
Epoxy glass	2.0×10^{9}	0.23	1800	Composite/soft
Wood (hard)	1.0×10^{10}	0.30	600	Natural material

5.2 We consider the initial displacement and velocity, which represent a standing wave in fundamental mode with a single impulse and shape deformation released from rest:
Initial displacement:

$$\phi(\mathrm{x,y},0) = \sin\left(\frac{\pi x}{L_x}\right) sin\left(\frac{\pi y}{L_y}\right) \quad (13)$$

Initial velocity:

$$\frac{\partial \phi(\mathrm{x,y,t})}{\partial t} = 0 \quad (14)$$

Where L_x and L_y are the lengths of the plate in the x and y-directions. They are keys geometric parameters defining the physical size of the rectangular plate and directly influences the vibration characteristics. The simulation solutions are presented in tabular form, 2D, and 3D plots of the surface for the Aluminium, Brass, Epoxy glass, and wood (hard), respectively.

Table 3. Numerical solutions for the various α when lengths of the plate are $L_x = 2$ and $L_y = 4$

(x, y)	Materials	$\alpha = 2.0$	$\alpha = 1.5$	$\alpha = 1.0$	$\alpha = 0.5$
0,0	Aluminium	0.0000000000	0.0000000000	0.0000000000	0.0000000000
	Brass	0.0000000000	0.0000000000	0.0000000000	0.0000000000
	Epoxy glass	0.0000000000	0.0000000000	0.0000000000	0.0000000000
	wood (hard)	0.0000000000	0.0000000000	0.0000000000	0.0000000000
0.2, 0.2	Aluminium	0.0483409082	0.0919498715	0.1283409081	0.1483409082
	Brass	0.0919498715	0.1265581407	0.2091949871	0.2911949871
	Epoxy glass	0.1265581407	0.1487780175	0.2211655814	0.3365581410
	wood (hard)	0.1487780173	0.1564344650	0.2977801734	0.3487781230
0.4, 0.4	Aluminium	0.0954915028	0.1267894518	0.1954915012	0.2836434465
	Brass	0.1816356325	0.2938926261	0.3216356320	0.3995491502
	Epoxy glass	0.2499999999	0.3090169943	0.3938926610	0.4616356320
	wood (hard)	0.2938926261	0.3619498715	0.4190169943	0.5111938926
0.6, 0.6	Aluminium	0.1402907797	0.1722464210	0.1970290779	0.2668489200
	Brass	0.2668489204	0.2954318731	0.3368489204	0.3972860295
	Epoxy glass	0.3672860297	0.4328761230	0.5672863421	0.6317706231
	wood (hard)	0.4317706236	0.6321654200	0.7367117706	0.8539904997
0.8, 0.8	Aluminium	0.1816356320	0.2454915021	0.3454915021	0.4321590169
	Brass	0.3454915028	0.4255282581	0.5755282581	0.6118778525
	Epoxy glass	0.4755282581	0.5590169990	0.6745159943	0.7122185080
	wood (hard)	0.5590169943	0.6877852522	0.8187785252	0.8920614028
1.0, 1.0	Aluminium	0.2185080127	0.3056269378	0.4156269356	0.5567249851
	Brass	0.4156269377	0.5120614420	0.6342178402	0.6761402817
	Epoxy glass	0.5720614026	0.6672498511	0.3724967851	0.7140281768
	wood (hard)	0.6724985119	0.7560710678	0.9707106781	0.9552825814

2D plots presentations.

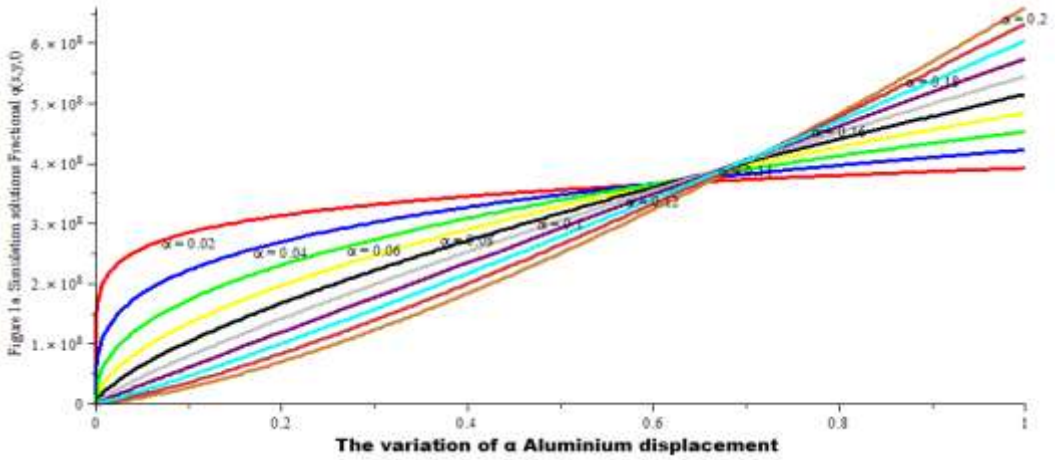

Figure 1a. Depict the trend of displacements ϕ(t) obtained for the various fractional derivatives of the four materials considered (Aluminium) the vibration dynamics in the rectangular thin plate model (1).

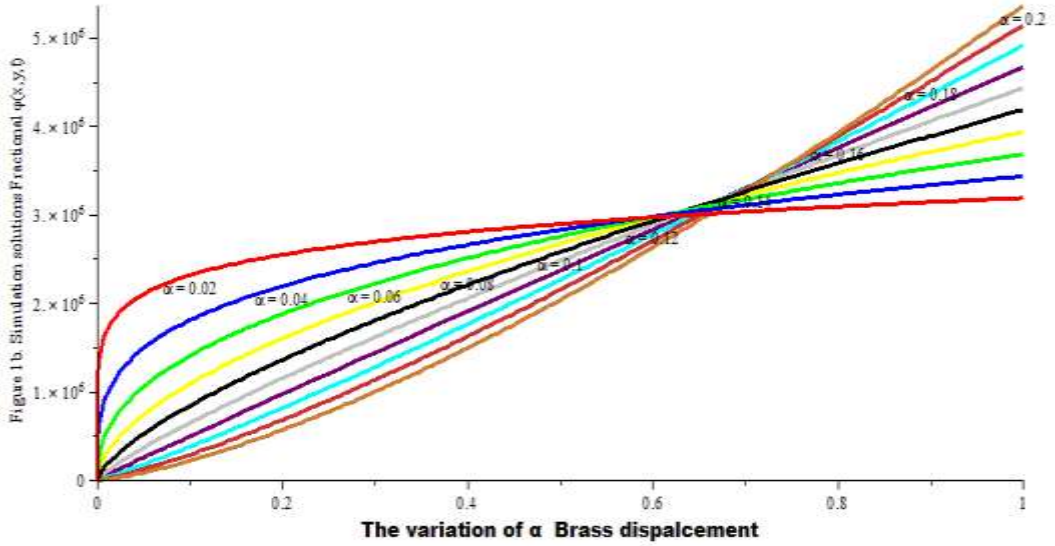

Figure 1b. Depict the trend of displacements ϕ(t) obtained for the various fractional derivatives of the four materials considered (Brass) the vibration dynamics in the rectangular thin plate model (1).

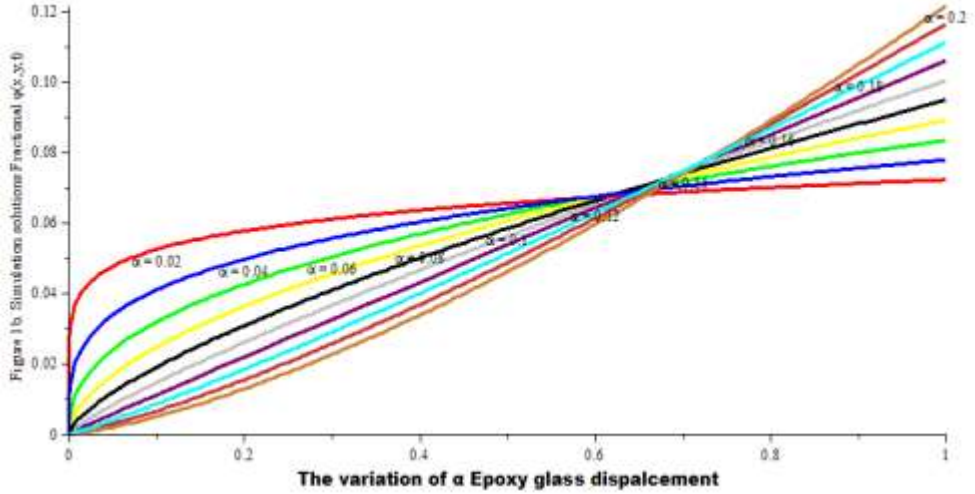

Figure 1c. Depict the trend of displacements ϕ(t) obtained for the various fractional derivatives of the four materials considered (Epoxy glass) the vibration dynamics in the rectangular thin plate model (1).

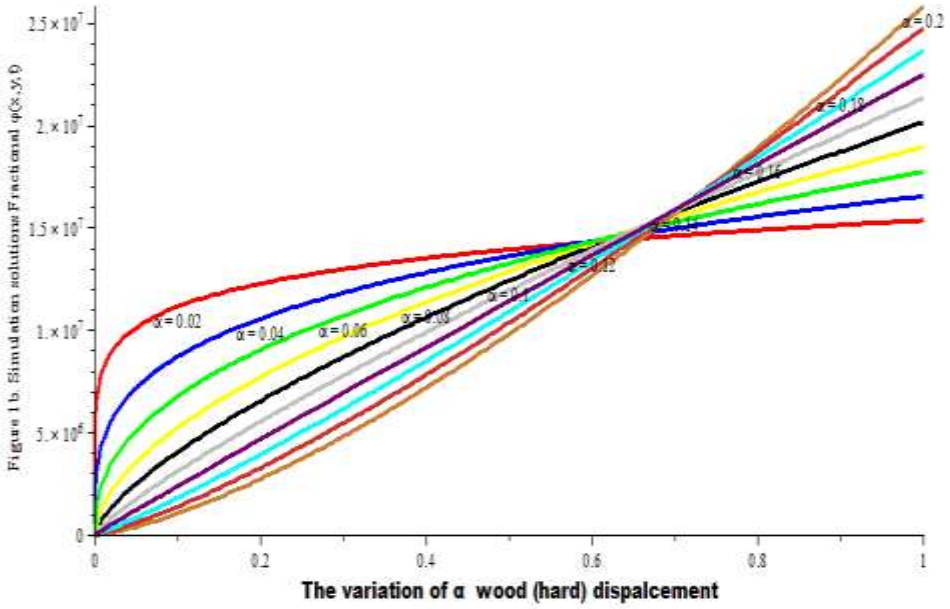

Figure 1d. Depict the trend of displacements ϕ(t) obtained for the various fractional derivatives of the four materials considered wood (hard) the vibration dynamics in the rectangular thin plate model (1)

3D plots presentations.

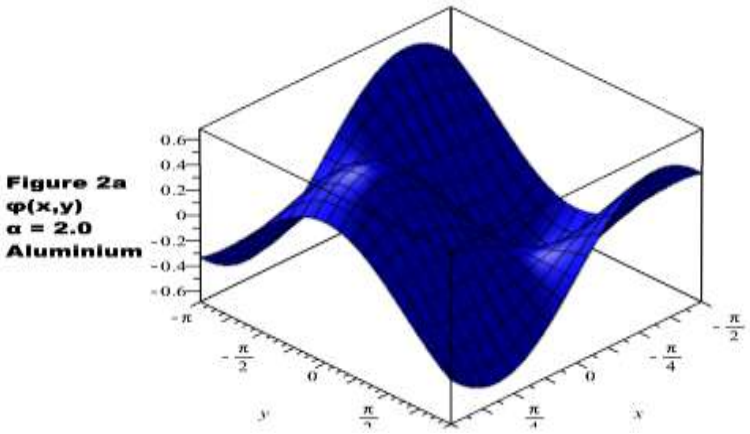

Figure 2a. Depict the trend of displacements ϕ(x,y) obtained for the classical derivatives of the four materials considered (Aluminium) for the vibration dynamics in the rectangular thin plate model (1)

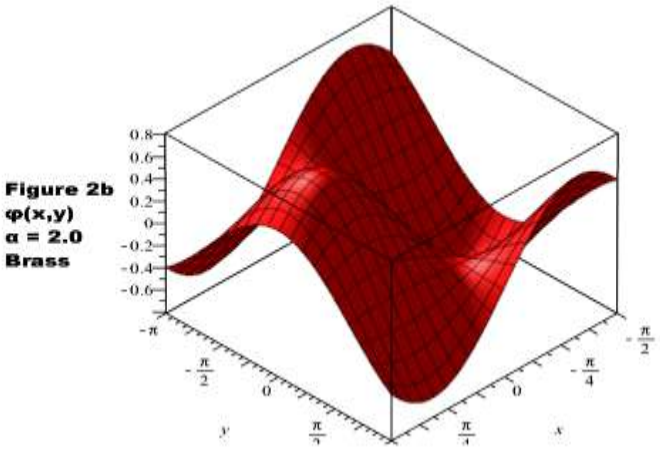

Figure 2b. Depict the trend of displacements ϕ(x,y) obtained for the classical derivatives of the four materials considered (Brass) for the vibration dynamics in the rectangular thin plate model (1).

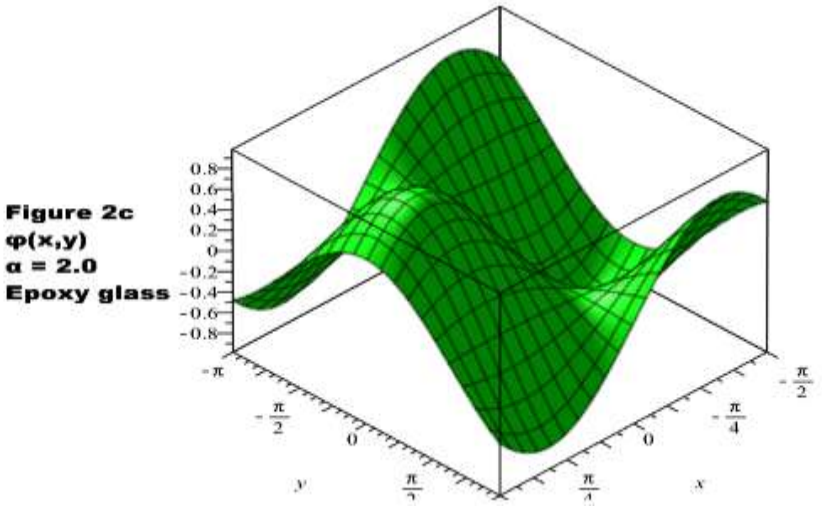

Figure 2c. Depict the trend of displacements ϕ(x,y) obtained for the classical derivatives of the four materials considered (Epoxy glass) for the vibration dynamics in the rectangular thin plate model (1)

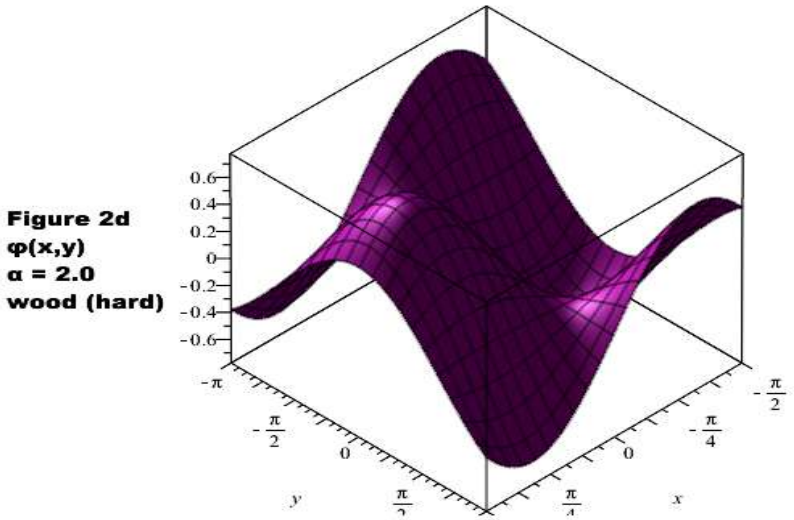

Figure 2d. Depict the trend of displacements ϕ(x,y) obtained for the classical derivatives of the four materials considered (wood (hard)) for the vibration dynamics in the rectangular thin plate model (1)

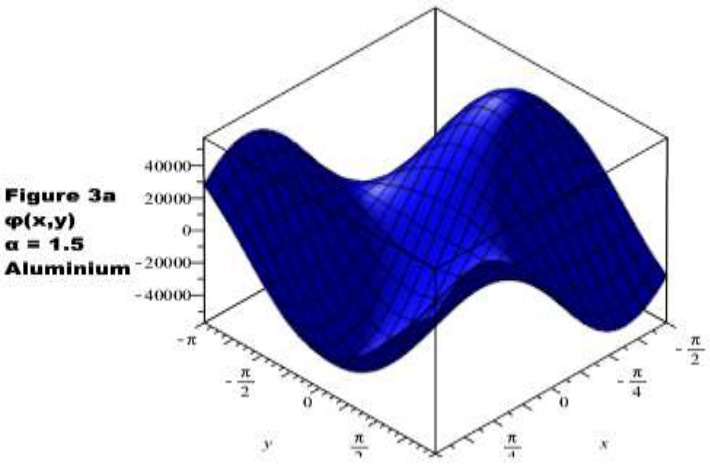

Figure 3a. Depict the trend of displacements ϕ(x,y) obtained for the fractional derivatives of the four materials considered (Aluminium,) for the vibration dynamics in the rectangular thin plate model (1).

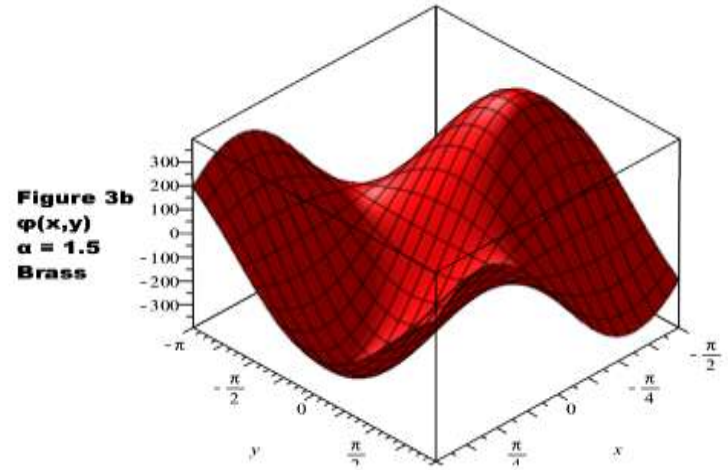

Figure 3b. Depict the trend of displacements ϕ(x,y) obtained for the fractional derivatives of the four materials considered (Brass) for the vibration dynamics in the rectangular thin plate model (1).

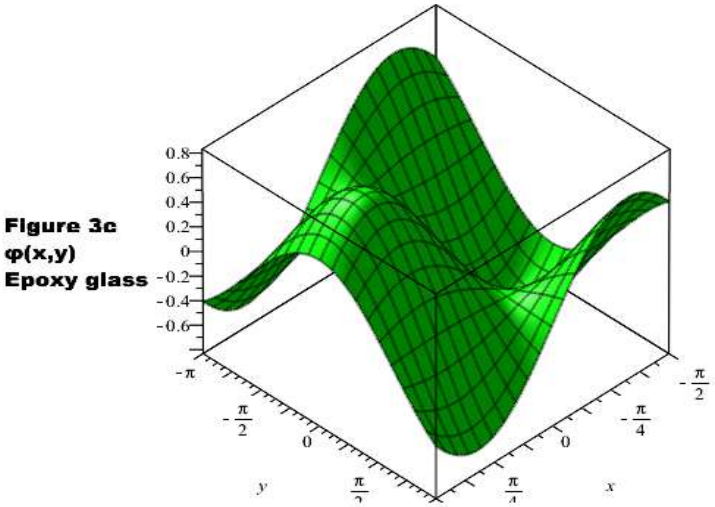

Figure 3c. Depict the trend of displacements ϕ(x,y) obtained for the fractional derivatives of the four materials considered (Epoxy glass) for the vibration dynamics in the rectangular thin plate model (1).

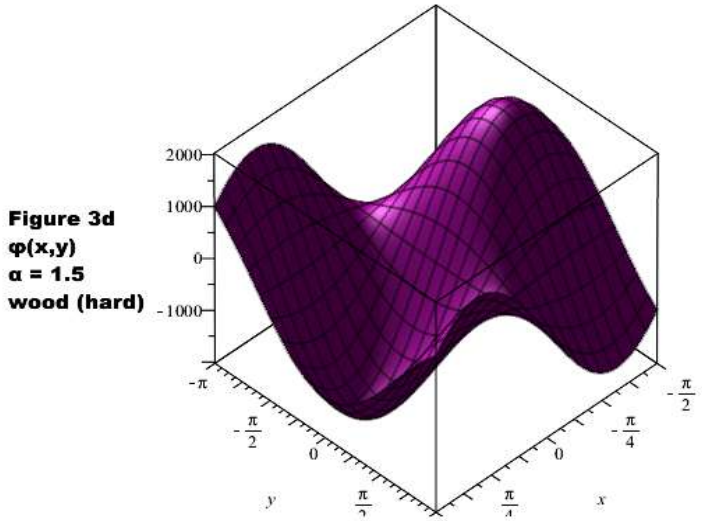

Figure 3d. Depict the trend of displacements ϕ(x,y) obtained for the fractional derivatives of the four materials considered (wood (hard)) for the vibration dynamics in the rectangular thin plate model (1).

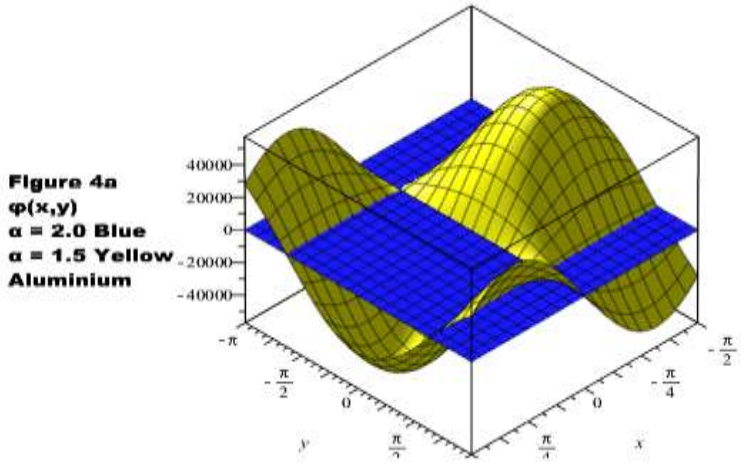

Figure 4a. Demonstrated the comparison of the displacements ϕ(x, y) obtained for the **integer derivative α=2.0** and **fractional derivative α=1.5** of the four materials considered (Aluminium) for the vibration dynamics in the rectangular thin plate model (1).

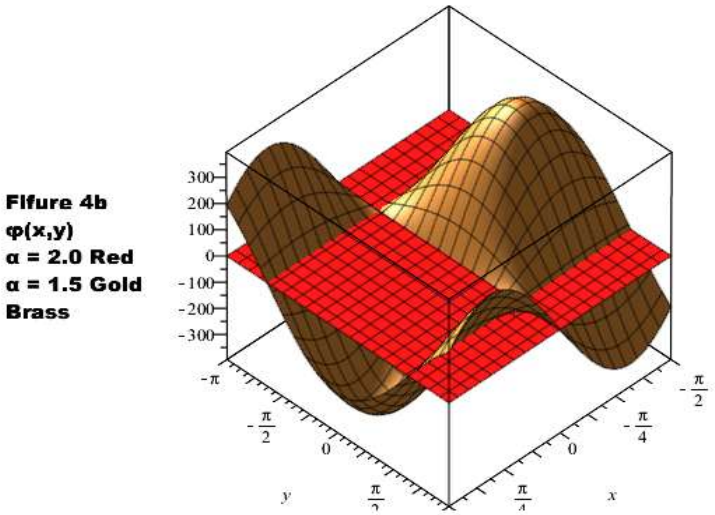

Figure 4b. Demonstrated the comparison of the displacements ϕ(x, y) obtained for the **integer derivative α=2.0** and **fractional derivative α=1.5** of the four materials considered (Brass) for the vibration dynamics in the rectangular thin plate model (1).

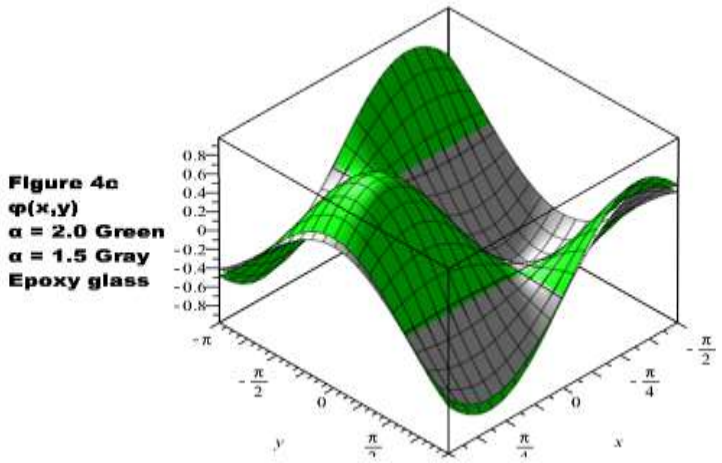

Figure 4c. Demonstrated the comparison of the displacements ϕ(x, y) obtained for the **integer derivative α=2.0** and **fractional derivative α=1.5** of the four materials considered (Epoxy glass) for the vibration dynamics in the rectangular thin plate model (1).

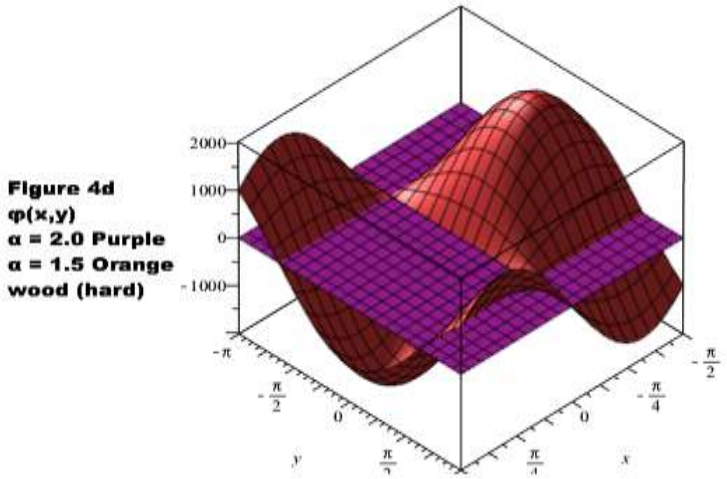

Figure 4d. Demonstrated the comparison of the displacements ϕ(x, y) obtained for the **integer derivative α=2.0** and **fractional derivative α=1.5** of the four materials considered (wood (hard)) for the vibration dynamics in the rectangular thin plate model (1).

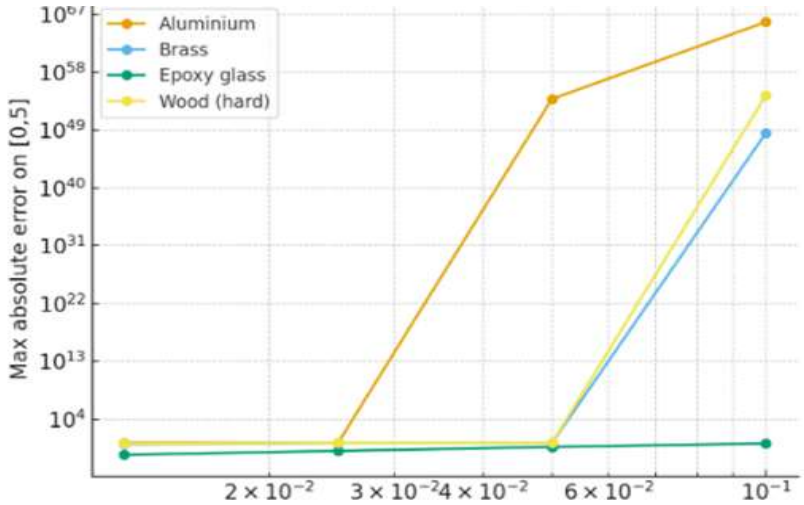

Figure 5. The convergence error analysis reveals that the numerical method's stability varies greatly with material properties. As shown in the log-log plot of max error vs ϕ(x), Aluminium exhibits severe divergence, where the error increases dramatically for larger time steps, indicating instability or poor suitability of the chosen scheme for highly conductive materials. Brass and Wood display similar but less extreme divergence. In contrast, Epoxy glass maintains low, stable error, highlighting its favorable numerical convergence under the given fractional-order model parameters.

RESULTS AND DISCUSSION

The finite difference scheme with a fractional time-stepping algorithm based on the Riemann-Liouville integral was employed to solve the vibration dynamics in a rectangular thin plate model and the numerical results presented in **Table 3** highlight clear differences in the dynamic response of the four materials under fractional-order thin-plate vibration. Across all coordinate points and fractional orders, Aluminium consistently shows the smallest displacement values, reflecting its high stiffness-to-density ratio and rapid decay of vibration. Hard wood generally follows, producing larger amplitudes than Aluminium but remaining lighter and more responsive than brass. Brass exhibits noticeably higher displacement values due to its high density, which slows vibrational decay despite having a relatively high modulus. Epoxy glass shows the largest responses at several points, especially for lower fractional orders, due to its low stiffness, making

it the most flexible material. As **α** decreases from 2.0 to 0.5, amplitude increases for all materials, confirming stronger memory effects in fractional systems. Overall, the comparison demonstrates that stiffer materials yield smaller responses and converge faster, while softer materials exhibit amplified fractional-order behaviour.

i. Figures 1a–1d depict 2D displacement evolutions of a thin plate under fractional-order vibration across four materials. Fractional derivatives crucially influence damping and memory effects, leading to varying maximal displacements: highest in Aluminium, moderate in Brass and Hard Wood, and minimal in Epoxy Glass due to strong viscoelastic damping.
ii. Figures 2a–2d show 3D displacement patterns of thin plates under classical dynamics (α=2) for Aluminium, Hard Wood, Brass, and Epoxy Glass. Material stiffness, density, and damping parameters shape vibration amplitude and distribution, guiding design for optimal damping and isolation.
iii. Figures 3a–3d show maximum displacements of a rectangular thin plate under fractional vibration dynamics (α=1.5) for Aluminium, Brass, Epoxy Glass, and Hard Wood. Displacement varies by material stiffness, density, and damping, with Aluminium highest, Epoxy Glass lowest, and Wood and Brass showing intermediate responses.
iv. Figures 4a–4d compare displacement responses using integer- and fractional-order derivatives for Aluminium, Brass, Epoxy Glass, and Hard Wood. Fractional derivatives produce higher vibration amplitudes due to damping and memory effects, while integer-order models predict lower amplitudes and altered frequencies, highlighting more realistic viscoelastic behavior.

CONCLUSION

This paper examined the fractional-order vibration dynamics of rectangular thin plates using a finite difference scheme combined with a fractional time-stepping algorithm based on the Riemann–Liouville integral. The results underscore the significant influence of fractional calculus on the mechanical behaviour of engineering materials, particularly in capturing memory-dependent and viscoelastic effects that classical integer-order models fail to represent adequately. By analysing four materials- Aluminium, Brass, Hard Wood, and Epoxy Glass-the study demonstrates how stiffness, density, and elastic properties govern their dynamic responses under fractional-order excitation. The numerical simulations reveal that Aluminium, due to its high stiffness-to-density ratio, consistently exhibits the smallest displacement amplitudes and the fastest decay of vibration. Hard Wood presents moderate vibrational responses, while Brass, with its high density, shows slower decay and larger amplitudes despite a relatively high modulus. Epoxy Glass remains the most flexible material, exhibiting the highest amplitudes, especially at lower fractional orders. The increased displacement associated with decreasing α highlights the strong memory and damping characteristics inherent in fractional-order systems. The convergence error analysis further reflects the relationship between material properties and numerical stability. While Aluminium and Brass display divergence under larger time steps, Epoxy Glass maintains stable convergence, making it more numerically compatible with the selected fractional-order scheme. These findings suggest that material behaviour must be carefully considered when applying fractional-order numerical methods to structural vibration problems. Graphical analyses from 2D and 3D displacement plots reinforce these conclusions, illustrating how fractional-order formulations yield more physically realistic behaviours than classical integer-order models. Overall, this paper provides a strong foundation for applying fractional calculus to advanced structural dynamics, enabling improved modelling of damping, energy dissipation, and viscoelasticity. The methodology and results offer valuable insights for material selection, vibration control, and structural design in engineering applications where memory effects play a crucial role.

REFERENCES

[1] Liu, J., Li, L., Peng, J., Chen, G., & Yang, D. (2023). Random vibration responses and reliability analyses of thin plates with geometric nonlinearity via direct probability integral method. *Springer Nature*, Vol. 111, pp. 11965–11987.

[2] Leng, B., Ullah, S., Tianlai, Y., & Kexin, L. (2022). New analytical free vibration solutions of thin plates using the Fourier series method. *Difference Equations*, Vol. 46, pp. 1–27.

[3] Rezvani, S. S., & Kiasat, M. S. (2018). Analytical and experimental investigation on the free vibration of a floating composite sandwich plate having viscoelastic core. *Arch. Civ. Mech. Eng.*, pp. 1–23.

[4] Ullah, S., Zhong, Y., & Zhang, J. (2019). Analytical buckling solutions of rectangular thin plates by straightforward generalized integral transform method. *Int. J. Mech. Sci.*, pp. 1–23.

[5] Qin, B., Zhong, R., Wu, Q., Wang, T., & Wang, Q. (2019). A unified formulation for free vibration of laminated plate through Jacobi-Ritz method. *Thin-Walled Structures*, pp. 1–23.

[6] Falade, K. I., Tiamiyu, A. T., & Tolufase, E. (2020). A study of thin plate vibration using homotopy perturbation algorithm. *International Journal of Engineering and Innovative Research*, Vol. 2(2), pp. 92–101.

[7] Sobamowo, M. G., Saheed, A., Salawu, A., Ahmed, A., & Yinusa, A. (2020). Application of Adomian decomposition method to free vibration analysis of thin isotropic rectangular plates submerged in fluid. *Journal of the Egyptian Mathematical Society*, Vol. 28(19), pp. 1–13.

[8] Avey, M., Kadioglu, S., Ahmetolan, N., & Fantuzzi, N. (2023). Mathematical modeling and solution of nonlinear vibration problem of laminated plates with CNT originating layers interacting with two-parameter elastic foundation. pp. 1–10.

[9] Sibtain, M., Yee, K., Shao Ong, O. Z., Mergen, H., Ghayesh, H., & Hussain, S. (2025). Poroelastic size-dependent dynamics of viscoelastic microbeams connected via a viscoelastic layer. *Mechanics Based Design of Structures and Machines*, Vol. 53(1), pp. 770–800.

[10] Mohamed, A. S., Mohamed, A., Eltaher, N., & Abo-bakr, R. M. (2024). Nonlinear dynamics and forced vibrations of simply-supported fractional viscoelastic microbeams using a fractional differential quadrature method. pp. 1–13.

[11] Miller, K. S., & Ross, B. (2003). *An Introduction to Fractional Calculus and Fractional Differential Equations*. John Wiley & Sons, New York, pp. 1–26.

[12] Callister, W. D., & Rethwisch, D. G. (2017). *An Introduction to Material Science and Engineering*. Wiley, pp. 234–264.